Landmark constrained non-rigid image registration with anisotropic tolerances

T. Lange[1], N. Papenberg[2], J. Olesch[2], B. Fischer[2] and P.M. Schlag[3]

[1] Experimental and Clinical Research Center (ECRC), Charite - Universitätsmedizin Berlin, Germany
[2] Insitute of Mathematics, University of Lübeck, Germany
[3] Charite Comprehensive Cancer Center (CCCC), Charite - Universitätsmedizin Berlin, Germany

Abstract— **The registration of medical images containing soft tissue like inner organs, muscles, fat , etc., is challenging due to complex deformations between different image acquisitions. Despite different approaches to get smooth transformations the number of feasible transformations is still huge and ambiguous local image contents may lead to unwanted results. The incorporation of additional user knowledge is a promising way to restrict the number of possible non-rigid transformations and to increase the probability to find a clinically reasonable solution. A small number of pre-operatively and interactively defined landmarks is a straight forward example for such expert knowledge. Typically, when vessels appear in the image data, a natural way is to determine landmarks as vessel branchings. Here, we present a generalization that allows also the usage of corresponding vessel segments. Therefor, we introduce a registration scheme that can handle anisotropic localization uncertainties. The contribution of this work is a consistent modeling of a combined intensity and landmark registration approach as an inequality constrained optimization problem. This guarantees that each reference landmark lies within an error ellipsoid around the corresponding template landmark at the end of the registration process. First results are presented for the registration of preoperative CT images to intra-operative 3D ultrasound data of the liver as an important issue in an intra-operative navigation system.**

Keywords— **non-rigid registration, inequality constrained optimization, landmarks, anisotropic tolerances, liver, 3D ultrasound**

I. Introduction

Non-rigid image registration is one of the key problems in computer-assisted oncological liver surgery. Based on preoperative CT data, resections are planned based on 3D models of the liver vessels and the tumor which are extracted from the image data [1]. During the intervention the surgeon is guided by a navigation system based on 3D ultrasound, which captures the current shape and position of the liver [2]. To transfer the preoperative plan to the patient on the operating table a non-rigid registration method is needed, which compensates liver deformations. The liver deformation arises from intra-operative bedding and from the mobilization of the organ.

There is only few work published regarding CT/MRI to ultrasound registration. Rigid methods have been presented, which are either intensity- [3], feature-based [4] or where the CT images are made similar to ultrasound images and then their correlation is measured [5]. Usually the liver vessels serve as features, because of their easy identification in CT/MRI and ultrasound data, in particular in Power Doppler ultrasound. Extensions of such vessel-based approaches to non-rigid transformations are described in [6, 7]. These methods, however, suffer from the problem that vessels cannot be extracted automatically from ultrasound data at high accuracy and speed. Alternatively, hybrid approaches [8, 9] fit preoperatively extracted features (vessels) directly to the intra-operative image data.

The incorporation of additional user knowledge into a non-rigid registration process is a promising topic in modern registration schemes to increase the robustness of the registration process. The combination of intensity based registration and some interactively chosen landmark pairs is a major approach in this direction [10, 11, 12, 13, 14]. As the interactive localization of point landmarks is always prone to errors, we introduce an inequality constrained optimization scheme, which guarantees corresponding landmarks to be at most a given distance apart from each other after registration. As the localization uncertainties might deviate in different directions we introduce for the first time a landmark constrained registration scheme with anisotropic tolerances (error ellipsoids), which can be used for the registration of vascular structures.

II. Methods

Given a reference image R (intra-operative 3D ultrasound) and a template image T (preoperative CT) with $R,T : \mathbb{R}^3 \to \mathbb{R}$ the aim of the registration process is to find a displacement vector field $y : \mathbb{R}^3 \to \mathbb{R}^3$, which transforms the domain of the template image in such a way, that corresponding points are mapped onto each other. In the general variational non-parametric image registration approach [15] a functional J depending on the transformation y is minimized. The functional consists of a distance measure $D[R,T(y)]$ quantifying the intensity differences of the reference R and the transformed template $T(y)$ and a regularizer $S[y]$ ensuring smooth and plausible transformations y . This leads to the following

O. Dössel and W.C. Schlegel (Eds.): WC 2009, IFMBE Proceedings 25/IV, pp. 2238–2241, 2009.
www.springerlink.com

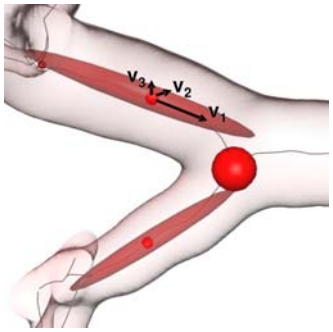

Fig. 1: Anisotropic segment and isotropic branching landmarks with eigenvectors v_1, v_2, v_3.

optimization problem:

$$\min_y J[y] = D[R, T(y)] + \alpha S[y]$$

with weighting factor $\alpha \in \mathbb{R}^+$. Different possibilities exist to incorporate corresponding landmark pairs $r_j, t_j \in \mathbb{R}^3, j = 1, \ldots, N$ into this intensity based registration approach. The first is to add a penalizer $P[y]$ to the functional [11] measuring the sum of the distances between the landmarks:

$$\min_y J[y] = D[R, T(y)] + \alpha S[y] + \beta P[y]$$

with weighting factor $\beta \in \mathbb{R}^+$. As the landmark misfit is globally controlled, the distance of individual landmarks might still be high after optimization. In addition the penalty approach suffers from parameter tuning (weighting factor β). An individual landmark control is possible by formulating a constrained optimization problem:

$$\begin{aligned} \min_y \quad & J[y] = D[R, T(y)] + \alpha S[y] \\ \text{subject to} \quad & C_j^{\text{eq}}[y] = 0, \quad j = 1, \ldots, N \end{aligned}$$

with three equality constraints $C_j^{\text{eq}}[y] = y(r_j) - t_j$ for each landmark pair [10, 12]. The exact mapping of corresponding landmarks onto each other is guaranteed in this scheme. But equality constraints are too restrictive because interactive landmark definition is always prone to errors. Here we are presenting a new approach by considering individual anisotropic landmark localization inaccuracies. As the localization uncertainty of a landmark might deviate in different directions (anisotropic errors) we define an ellipsoidal tolerance volume for each landmark pair by a weighted norm [16]:

$$C_j^{\text{iq}}[y] = 1 - \left\| y(r_j) - t_j \right\|_{W_j}^2 = 1 - (y(r_j) - t_j) W_j (y(r_j) - t_j)$$

with $W_j \in \mathbb{R}^{3\times 3}$ being positive definite symmetric weighting matrices. The resulting inequality constrained optimization problem looks like:

$$\begin{aligned} \min_y \quad & J[y] = D[R, T(y)] + \alpha S[y] \\ \text{subject to} \quad & C_j^{iq}[y] \geq 0, \quad j = 1, \ldots, N \end{aligned} \tag{1}$$

In [17] also an anisotropical landmark weighting is used, but in a penalizer scheme with the above mentioned disadvantages.

The anisotropically weighted landmarks yield a higher flexibility in defining landmark pairs. For example instead of using point landmarks at corresponding liver vessel branchings, which are usually difficult to identify in 3D, also landmarks between two corresponding branchings (vessel segments) can be used, which are often easier to identify. With the latter landmarks the localization uncertainty is high along the vessel, but low perpendicular to it (see Fig. 1). The covariance of the anisotropic localization uncertainty can be modeled via their eigenvalues and eigenvectors. The first eigenvector $v_1^j \in \mathbb{R}^3$ points in the direction of the corresponding vessel at the position of the landmark, the other two eigenvectors $v_2^j, v_3^j \in \mathbb{R}^3$ are perpendicular to it. As the localization uncertainty is high in the direction of the vessel and low perpendicular to it depending on the area of the vessel cross section, the eigenvalues are chosen as $\lambda_1^j = 5r_j^2, \lambda_2^j = r_j^2, \lambda_3^j = r_j^2$, with r_j being a radius estimation of the vessel at landmark j. The radii are already available due to the preoperative modeling of the vessels for the surgery planning process. With $D_j = \text{diag}(\lambda_1^j, \lambda_2^j, \lambda_3^j)$ and $V_j = (v_1^j, v_2^j, v_3^j)$ the uncertainty matrices are defined as:

$$\Sigma_j = V_j^T D_j V_j.$$

The weighting matrices are then the inverse of the covariance matrices: $W_j = \Sigma_j^{-1}$. The approach can be seen as a generalization of the isotropic tolerance method described in [14]. To handle such isotropic tolerances the matrix Σ is choosen as $\Sigma_j = a_j^2 I_3$, with $a_j \in \mathbb{R}^+$ being the radius of an error sphere around landmark j.

For the optimization of (1) we use the *first-discretize-then-optimize-approach*. That means, the objective function as well as the constraints are discretized first to achieve a finite constrained optimization problem. In particular, the constraints are approximated by means of linear interpolation as described in [12]. Analytical gradients for the discretized problem are determinable allowing efficient optimization schemes. We solve the finite optimization problem by a generalized Gauss-Newton-method [18].

III. Results

We show the effectiveness of the proposed registration scheme on an illustrative example, which is a simplified geometry of portal veins in a real liver CT containing only the biggest vessels. A realistic deformation based on a combined intensity and landmark registration with equality constraints of clinical CT and 3D ultrasound data is determined. The landmarks have been defined on vessel branchings. This deformation is applied to the example image to get an artificial template. In the first row of Fig. 2 the vessels extracted from the template and reference image as well as the landmarks and vessel center lines are shown. The points on the center lines are displaced by 5 ± 2mm. 6 landmark pairs have been interactively chosen on the vessel segments. Landmark 3 has been moved by $10mm$ in the direction of the vessel.

We chose the curvature regularizer $S^{\text{curv}} = \frac{1}{2}\int \sum_{k=1}^{3} \left\|\Delta(y_k - y_k^0)\right\|^2 dx$ [15] with y^0 being the initial displacement field and the sum of squared differences (SSD) as the distance measure $D^{\text{SSD}} = \frac{1}{2}\int (T(y(x)) - R(x))^2 dx$ because in our example the vessels appear bright compared to the background in template and reference image. We used a multilevel and multi-resolution strategy for the images T, R and the displacement field y. We started on a grid with 7.5 mm spacing and refined twice to a final spacing of 1.9mm. The original resolution of the images was $1 \times 1 \times 1mm^3$.

As can be seen in the second and third row of Fig. 2 the isotropic tolerance at landmark 3 is to restrictive to compensate the displacement of the landmark, but the anisotropic tolerance is suitable for compensation while keeping the restrictive tolerance perpendicular to the vessel.

IV. Discussion and Conclusion

Different ways have been published recently to combine intensity and landmark information in a joint registration process even for landmarks with anisotropic uncertainties. The contribution of this work is a consistent modeling as an inequality constrained optimization problem guaranteeing that each reference landmark lies within an error ellipsoid around the corresponding template landmark at the end of the registration process. In contrast to [17] the anisotropically weighted landmark differences are not added as a penalizer to the registration functional, but as hard inequality constraints. In addition not an alternating optimization scheme, but a direct optimization scheme has been implemented. The presented algorithm is a generalization to the one published by Papenberg et al. [14] with isotropic spherical landmark tolerances.

Vessel segment landmarks with anisotropic localization uncertainties are a promising alternative and/or extension to vessel branching landmarks with isotropic localization uncertainties. They offer an additional flexibility for the interactive definition of landmarks on vessel trees allowing for an intuitive and efficient registration workflow. The first results on an illustrative but realistic example are promising such that the next step will be a thorough and quantitative investigation on a significant number of clinical data sets from patients, which underwent computer assisted liver surgery.

References

1. Selle D, Preim B, Schenk A, Peitgen HO. Analysis of vasculature for liver surgical planning *IEEE Trans Med Imaging.* 2002;21:1344–1357.
2. Beller S, Hünerbein M, Eulenstein S, Lange T, Schlag PM. Feasibility of navigated resection of liver tumors using multiplanar visualization of intraoperative 3D ultrasound data *Ann Surg.*. 2007;246:288–294.
3. Roche A, Pennec X, Malandain G, Ayache N. Rigid Registration of 3-D Ultrasound With MR Images: A New Approach Combining Intensity and Gradient Information *IEEE Trans Med Imag.* 2001;20:1038–1049.
4. Penney GP, Blackall JM, Hamady MS, Sabharwal T, Adam A, Hawkes DJ. Registration of freehand 3D ultrasound and magnetic resonance liver images *Med. Image Anal.*. 2004;8:81–91.
5. Wein W, Brunke S, Khamene A, Callstrom MR, Navab N. Automatic CT-ultrasound registration for diagnostic imaging and image-guided intervention *Med Imag Anal.* 2008;12:577–585.
6. Lange T, Eulenstein S, Hünerbein M, Schlag PM. Vessel-based non-rigid registration of MR/CT and 3D ultrasound for navigation in liver surgery *Comput Aided Surg.* 2003;8:228–240.
7. Reinertsen I, Descoteaux M, Siddiqi K, Collins DL. Validation of vessel-based registration for correction of brain shift *Medical Image Analysis.* 2007;11:374–388.
8. Aylward SR, Jomier J, Weeks S, Bullitt E. Registration and Analysis of Vascular Images *Int J Comput Vision.* 2003;55:123–138.
9. Lange T, Lamecker H, Hünerbein M, Eulenstein S, Beller S, Schlag PM. A distance measure for non-rigid registration of geometrical models to intensity data in *CARS*;2 (Supple 1) of *IJCARS*:204–206 2007.
10. Fischer B, Modersitzki J. Combination of automatic non-rigid and landmark based registration: the best of both worlds in *Medical Imaging 2003: Image Processing*;5032 of *SPIE*:1037–1048 2003.
11. Papenberg N, Lange T, Modersitzki J, Schlag PM, Fischer B. Image registration for CT and intra-operative ultrasound data of the liver in *SPIE Medical Imaging: Visualization, Image-guided Procedures, and Modeling*;6918:691808 2008.
12. Lange T, Papenberg N, Heldmann S, Modersitzki J, Fischer B, Schlag PM. 3D ultrasound-CT registration of the liver using combined landmark-intensity information *IJCARS.* 2009;4:79-88.
13. Olesch J, Papenberg N, Lange T, Conrad M, Fischer B. Matching CT and ultrasound data of the liver by landmark constrained image registration in *SPIE Medical Imaging: Visualization, Image-guided Procedures, and Modeling*;7261:72610GSPIE 2009.
14. Papenberg N, Olesch J, Lange T, Schlag PM, Fischer B. Landmark constrained non-parametric image registration with isotropic tolerances in *Bildverarbeitung für die Medizin (BVM)*:122–126 2009.
15. Modersitzki J. *Numerical Methods for Image Registration*. Oxford University Press 2004.
16. Rohr K, Stiehl H, Sprengel R, Buzug T, Weese J, Kuhn M. Landmark-Based Elastic Registration Using Approximating Thin-Plate Splines *IEEE Trans Med Imag.* 2001;20:526–534.
17. Wörz S, Rohr K. Hybrid Physics-Based Elastic Image Registration Using Approximating Splines in *SPIE Med Imag.: Imag. Process.* 2008.
18. Bock HG, Kostina E, Schlöder JP. Numerical Methods for Parameter Estimation in Nonlinear Differential Algebraic Equations in *GAMM Mitt.*;30:376–408 2007.

Fig. 2: In the first column reference (grey) and template (red) vessels are shown. In the second row the error ellipsoids around template landmarks as well as the position of reference landmarks is visualized. In addition the vessel center lines are shown. In the first row the original deformed vessels and landmark positions are presented. Landmark 3 is displaced in the direction of the vessel. In the second row registration results using isotropic tolerances around the landmarks and in the third row using anisotropic tolerances are visualized